LETTER

https://doi.org/10.1038/s41586-018-0126-y

Late-surviving stem mammal links the lowermost Cretaceous of North America and Gondwana

Adam K. Huttenlocker[1]*, David M. Grossnickle[2], James I. Kirkland[3,4], Julia A. Schultz[5] & Zhe-Xi Luo[2,5]*

Haramiyida was a successful clade of mammaliaforms, spanning the Late Triassic period to at least the Late Jurassic period, but their fossils are scant outside Eurasia and Cretaceous records are controversial[1–4]. Here we report, to our knowledge, the first cranium of a large haramiyidan from the basal Cretaceous of North America. This cranium possesses an amalgam of stem mammaliaform plesiomorphies and crown mammalian apomorphies. Moreover, it shows dental traits that are diagnostic of isolated teeth of supposed multituberculate affinities from the Cretaceous of Morocco, which have been assigned to the enigmatic 'Hahnodontidae'. Exceptional preservation of this specimen also provides insights into the evolution of the ancestral mammalian brain. We demonstrate the haramiyidan affinities of Gondwanan hahnodontid teeth, removing them from multituberculates, and suggest that hahnodontid mammaliaforms had a much wider, possibly Pangaean distribution during the Jurassic–Cretaceous transition.

The ecological expansion of crown Mammalia accelerated in the wake of extinctions of diverse and disparate archaic mammaliamorph groups during the mid-Mesozoic[1]. Haramiyidans represent one such clade of early mammaliamorphs that show preservation of notable links between nonmammalian and mammalian structure and physiology[2–4]. Their fossils, which were dated to the Late Triassic–Jurassic, were historically limited to isolated teeth and incomplete gnathal remains[4,5], hindering a more complete understanding of their radiation. Recent discoveries of articulated skeletal material of eleutherodont haramiyidans from the Middle–Upper Jurassic of China have shed new light on their diversification[6,7], although these fossils have also sparked new debate over their phylogenetic position[4,6–12].

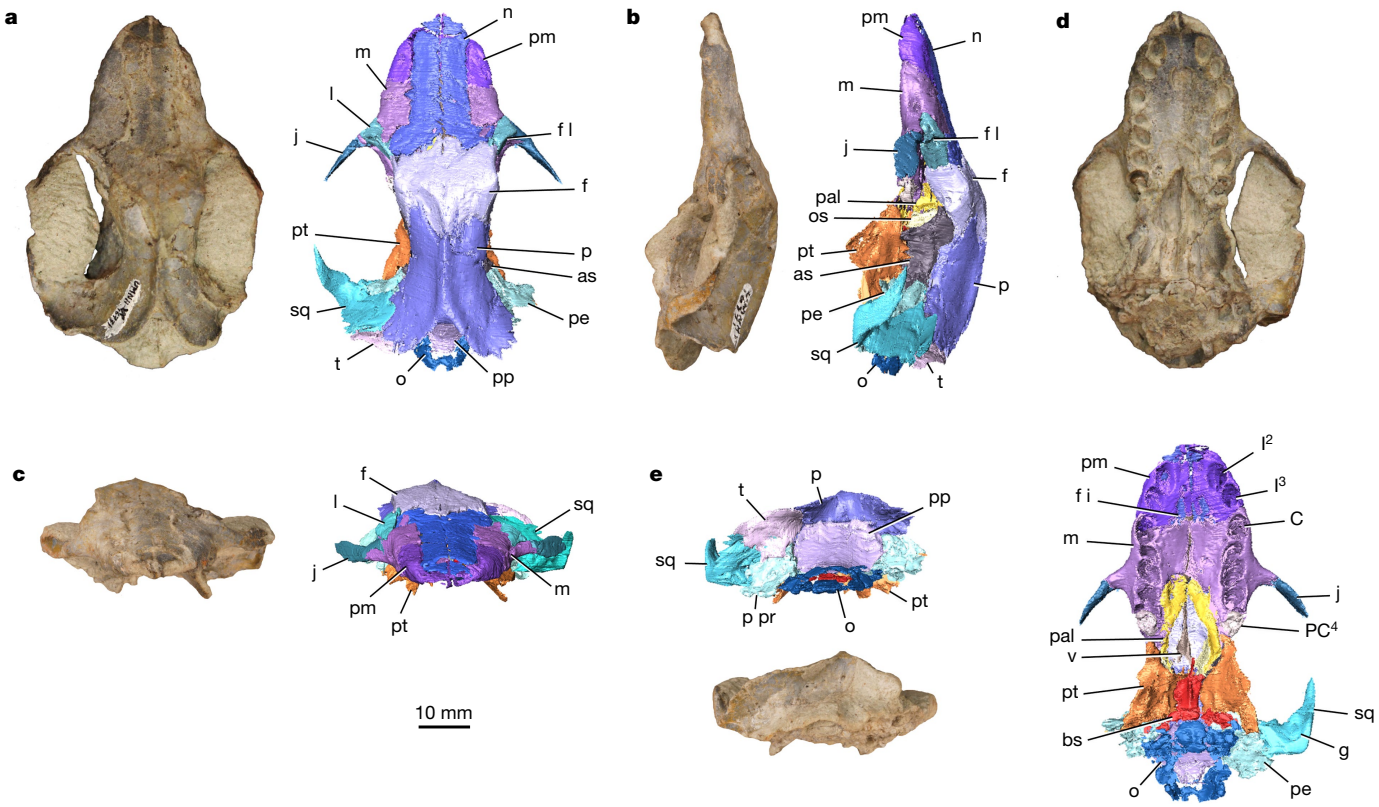

Fig. 1 | Cranium of *C. wahkarmoosuch*. **a**–**e**, Holotype in dorsal (**a**), left lateral (**b**), frontal (**c**), ventral (**d**) and occipital (**e**) views. as, alisphenoid (epipterygoid); bs, basisphenoid; C, upper canine alveolus; f, frontal; f i, incisive foramen; f l, lacrimal foramen; g, squamosal glenoid; I^2, first upper incisor alveolus (homologous to second incisor position in earlier haramiyidans); I^3, second upper incisor alveolus (homologous to third incisor position); j, jugal; l, lacrimal; m, maxilla; n, nasal; o, occipital; os, orbitosphenoid; p, parietal; p pr, paroccipital process; pal, palatine; PC^4, in situ posterior upper postcanine (molar); pe, petrosal; pm, premaxilla; pp, postparietal; pt, pterygoid; sq, squamosal; t, tabular; v, vomer.

[1]Department of Integrative Anatomical Sciences, University of Southern California, Los Angeles, CA, USA. [2]Committee on Evolutionary Biology, The University of Chicago, Chicago, IL, USA. [3]Utah Geological Survey, Salt Lake City, UT, USA. [4]Natural History Museum of Utah, Salt Lake City, UT, USA. [5]Department of Organismal Biology and Anatomy, The University of Chicago, Chicago, IL, USA. *e-mail: ahuttenlocker@gmail.com; zxluo@uchicago.edu

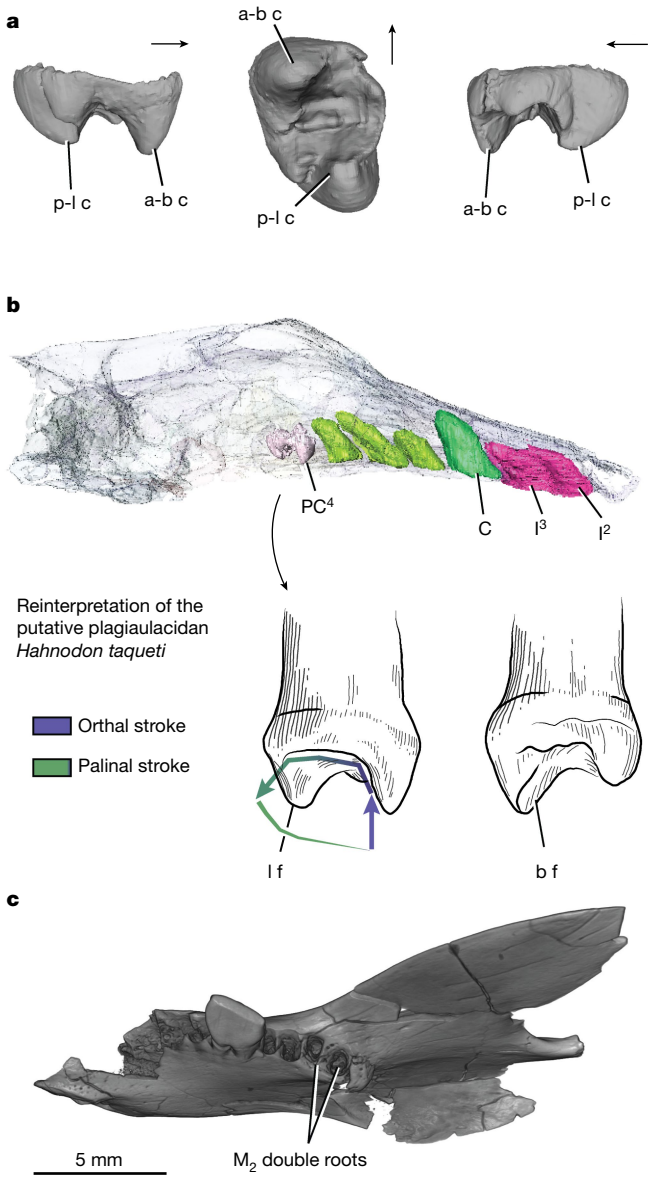

Fig. 2 | Dentition of *Cifelliodon*. **a**, Right posterior molar in buccal (left), occlusal (middle) and lingual (right) views. Arrows denote anterior. **b**, Reinterpretation of *Hahnodon*. Roots and posterior molar of *Cifelliodon* (top) shown for comparison. Note that *Hahnodon* in **b** does not match completely divided M_2 roots of multituberculates (**c**) (*Paulchoffatia*, GUI MAM 8/73). Images are not to scale. *Hahnodon* redrawn from previous publications[14, 21]. a-b c, anterobuccal cusp; b f, anterobuccal furrow; I, incisor position (homologous positions to earlier haramiyidans); l f, posterolingual furrow; M_2, second lower molar; p-l c, posterolingual cusp; PC^4, fourth postcanine (posterior molar).

Haramiyidans have frequently been included with multituberculates in 'Allotheria', a disputed taxonomic grouping that was diagnosed by dentition, with molars that have multiple cusp rows and palinal (anteroposterior) motion during mastication[4, 6, 9]. The limited overlapping morphology that is available in eleutherodonts and earlier haramiyidans (for example, *Thomasia* and *Haramiyavia*), coupled with a sparse fossil record, complicates our ability to resolve the group's global radiation and purported relationships to multituberculates. Here, we report an exceptionally preserved cranium from the basal Cretaceous of Utah, USA, that fills substantial morphologic and spatiotemporal gaps in our understanding of this important group. The specimen provides the basis of a new genus and species.

Mammaliaformes sensu Rowe (1986)[13]
Haramiyida Hahn, Sigogneau-Russell and Wouters (1989)[2]
Hahnodontidae Sigogneau-Russell (1991)[14]
Cifelliodon gen. nov.
Cifelliodon wahkarmoosuch sp. nov. (Fig. 1)

Etymology. Cifelli's tooth (Latin: -odon) of the Yellow Cat (Ute language: yellow, wahkar; cat, moosuch). Genus name honours Richard Cifelli for his contributions to Cretaceous mammal research in the American West.

Holotype. An exceptionally preserved skull, UMNH VP 16771 (Natural History Museum of Utah, Vertebrate Paleontology Collection).

Locality and horizon. The holotype is from the 'Andrew's Site' quarry in the Lower Cretaceous Yellow Cat Member, Cedar Mountain Formation, Grand County, Utah, USA[15] (Extended Data Fig. 1). Radiometric dating places the age between approximately 139 and 124 million years old (see Methods and Supplementary Information).

Diagnosis. Medium-to-large Mesozoic mammaliaform with broad, shallow skull and rostrum and a reduced marginal tooth count; dental formula: I2:C1:PC4; ultimate upper molars with high anterobuccal cusp and low, broad posterolingual cusp connected by a low ridge; septomaxilla absent; incisive foramina enlarged and positioned posteriorly on palate behind the level of the last (posterior) incisor pair; massive pterygoid transverse process that extends far ventral to the palatal surface; attenuated lacrimal anterior process with limited nasolacrimal contact; prominent sagittal crest; extensive occipital exposure of parietal and postparietal; plesiomorphic retention of a tabular bone; differs from *Hahnodon* in its larger size and higher aspect ratio of the rear molar in occlusal view (slightly more triangular than oval, with posterior apex).

Description. The skull of *Cifelliodon* (Fig. 1 and Extended Data Figs. 2–5) is large relative to other Mesozoic mammaliaforms (basal length around 70 mm; estimated body mass 0.91–1.27 kg)[16, 17] (see Methods and Supplementary Information). The upper dentition is largely missing, but preserves alveoli for two incisors, one canine and four postcanine maxillary teeth, including an in situ, unerupted ultimate molar pair (Fig. 2). The incisor roots were strongly posteriorly reclined and converged medially, suggesting procumbency as in haramiyidans, some multituberculates and gondwanatheres—another enigmatic group of mainly herbivorous mammal relatives that was restricted to Gondwana and has sometimes been classified as 'allotheres'[18, 19]. The postcanine alveoli have approximately the same diameter as the canine alveolus and are also 'undivided' and reclined more posteriorly. The ultimate molar preserves a distinctive central valley that is closed-off anteriorly by a tall antero-buccal cusp and lingual ridge that connects to a lower posterolingual cusp, a pattern analogous to that of the fruit-eating hammer-headed bat *Hypsignathus monstrosus*[20]. Other haramiyidans shared a similar configuration with a chewing cycle that had both orthal and palinal movements[4], but their upper molars differed in that the posterior cusp is larger than the anterior. In this regard, the ultimate molar of *Cifelliodon* is a closer analogue to *Hypsignathus* than that of other haramiyidans, and, except for its larger size and proportional differences, is nearly identical to an isolated tooth from the Lower Cretaceous of Morocco previously regarded as a multituberculate lower molar (M_2): *Hahnodon taqueti*[14, 21]. Here, we regard the assignment of *Hahnodon* to multituberculates as problematic because, similar to *Cifelliodon*, the molar morphology includes a prominent antero-buccal cusp that is uncharacteristic of plagiaulacidan multituberculate M_2s, a central valley that is closed off anteriorly and incompletely divided roots (multituberculates display completely bifurcated roots; Fig. 2c). Other authors have also questioned the multituberculate affinity of hahnodontid teeth, tentatively suggesting that they be moved to Haramiyida[5].

The skull shares additional features with some haramiyidans: upper incisor alveoli deep with procumbent orientation (Extended Data Figs. 6–8); lower canine fossa on maxilla-premaxilla absent; upper incisor number reduced to fewer than three; and upper postcanine loci reduced to five or fewer[4, 9] (Extended Data Table 1). Moreover, *Cifelliodon* retains

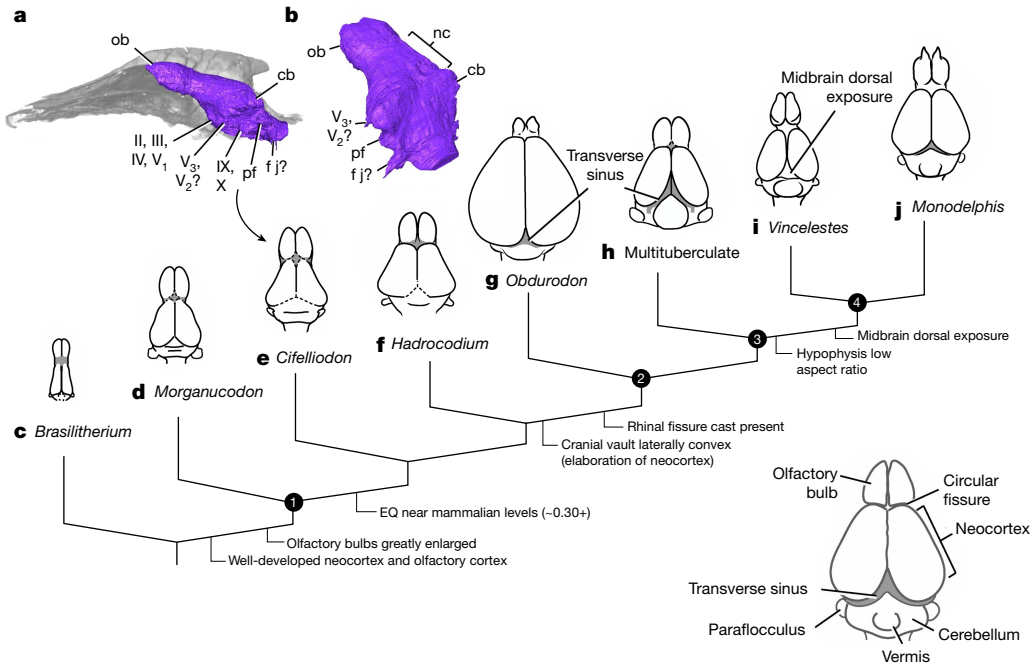

Fig. 3 | Brain endocast in *Cifelliodon* and other mammaliamorphs. **a**, **b**, Endocast of *Cifelliodon* in left lateral (**a**) and posterior oblique (**b**) views. **c**, Cynodont *Brasilitherium*[29]. **d**, Mammaliaform *Morganucodon*[22]. **e**, Hahnodontid mammaliaform *Cifelliodon*. **f**, *Hadrocodium*[22]. **g**, Monotreme *Obdurodon*[22]. **h**, Multituberculate (based on *Chulsanbaatar*)[22]. **i**, *Vincelestes*[23]. **j**, *Monodelphis*[30]. Drawings scaled to their relative encephalization quotients (EQ). Major nodes are: (1) Mammaliaformes, (2) Mammalia, (3) Theriiformes, (4) Cladotheria (therians and close allies). cb, cerebellar hemisphere; f j, jugular foramen cast in perilymphatic fossa; nc, neocortex region; ob, olfactory bulb; pf, parafloccculus cast; II, III, IV, V_1, cranial nerve exits near sphenorbital fissure; V_3, V_2, mandibular (and maxillary?) trigeminal branch roots; IX, X, glossopharyngeal and vagus nerve roots.

several plesiomorphic traits seen in Triassic mammaliamorphs, but not exhibited widely by previously known Cretaceous mammals, including: parietal lateral margins waisted rather than bulging outward; tabular bone present (also in the gondwanathere *Vintana*); pterygopalatal ridges present (also in select theriiforms, including cimolodontan multituberculates[19]); pterygoid flanges massive; secondary palate posterior limit well anterior to level of ultimate molar; maxilloturbinal supporting ridges absent on internal surface of maxilla; palatine anterodorsal expansion modest, such that maxilla and frontal maintain contact on anteromedial wall of orbit; and anterior part of the jugal extends to the facial part of the maxilla and forms a part of the anterior orbit. Nevertheless, the specimen also exhibits crown mammal features, including: a premaxilla facial process that is extensive and borders on the nasal; premaxilla with reduced internarial process; and posterior portion of jugal that terminates well anterior to the squamosal glenoid.

High-resolution X-ray computed tomography reveals an endocranial morphology that is transitional between earlier stem mammals and crown Mammalia (Fig. 3). The cranial vault is relatively modest in size (encephalization quotient 0.25–0.30; following a previously published method[22]), smaller than in the mammaliaform *Hadrocodium* (approximately 0.50) and some Cretaceous crown mammals (for example, *Vincelestes*, 0.37; *Pucadelphys*, 0.32)[22,23]. Much of the enlargement in brain volume was formed by the massive olfactory bulbs and piriform cortex as in other early mammaliaforms. Given the medially waisted parietals and limited endocranial capacity, there was little expansion of the neocortex. The endocast surface is largely lissencephalic, olfactory bulbs massive and a shallow peduncle in place of the circular fissure, thus showing poor gross differentiation of neocortical structures. This contrasts with early therians and other crown mammals more typical of the Cretaceous that show greater differentiation of neocortical structures and their boundaries in endocasts (Fig. 3). Many posterior endocranial structures that are visible on the endocast (perilymphatic foramen cast, parafloccular cast) are located at about the level of the wide, shallow glenoid fossa as in other early mammaliaforms, but not as posteriorized as in large-brained therians. As in other early mammaliaforms, the endocranium of *Cifelliodon* supports the premise that haramiyidans exhibited a similar degree of encephalization and behavioural complexity that was driven mainly by olfaction[22].

We assessed the phylogenetic position of *Cifelliodon* and Haramiyida using an updated morphological character matrix[4,24]. Broad-level relationships support that Haramiyida is monophyletic and represents a close sister group to Mammalia[4,24], rather than a paraphyletic assemblage of crown mammals related to multituberculates (in contrast to Zheng et al.[6]) (Fig. 4 and Extended Data Fig. 9). We define Haramiyida as all mammaliaforms more closely related to *Thomasia* and *Haramiyavia* than to *Didelphis*. Within Haramiyida, *Cifelliodon* forms a relationship with *Hahnodon* in a polytomy with the gondwanathere *Vintana*[18]. However, the position of gondwanatheres is only weakly supported; for example, an alternate tree topology constraining *Vintana* to a sister taxon relationship with multituberculates results in a tree score that is only nine steps longer than our most parsimonious tree (Templeton test, $P = 0.139$). However, support for a monophyletic Haramiyida outside crown Mammalia is significantly more robust than moving the clade into crown mammals along with *Vintana* and multituberculates (as in the previously published topology[18]), which requires 24 additional steps ($P = 0.032$).

Although the haramiyidan affinity of hahnodontids has been tenuous in the absence of more complete fossils, the exceptional preservation of *Cifelliodon* helps to strengthen the group's relationship to Haramiyida while revising its biogeographic history. *Cifelliodon* supports that haramiyidan stem mammals survived into the Early Cretaceous and sustained broad distributions in Laurasia and Gondwana, bridging Jurassic and Cretaceous terrestrial ecosystems across continents. The only previous haramiyidan material of Gondwanan origin included the isolated dentition of *Allostaffia* from the Jurassic of Tanzania[25] and *Avashishta*—an isolated molar of uncertain affinities from the Upper Cretaceous of India[26]. The further presence of hahnodontids in North America and Africa mirrors underappreciated Pangaea-wide occurrences of Cretaceous tetrapods, including several shared dinosaurian taxa[27,28] that linked northern and southern continents much later than previously recognized (see Supplementary Information).

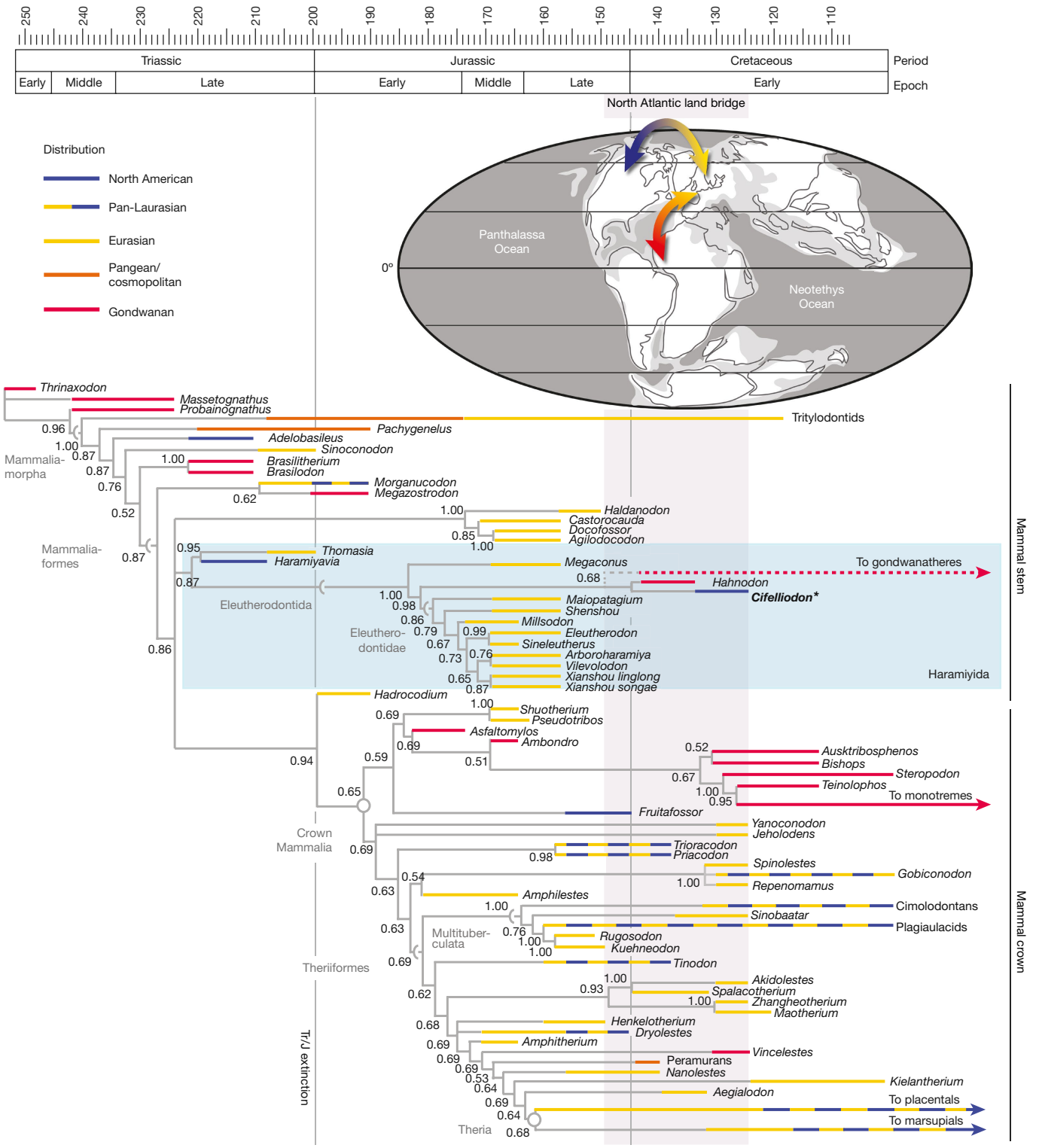

Fig. 4 | Time-calibrated phylogeny and biogeography of Mesozoic mammaliamorphs. Bayesian consensus cladogram for the analysis of 125 mammalian and nonmammalian synapsid taxa and 538 morphological characters. Note that haramiyidan stem mammals, previously restricted to Laurasia in the Jurassic period, exhibited distributions into Gondwana by the Cretaceous period. Cretaceous nonmammalian mammaliamorphs were rare, but globally widespread. Values at the nodes represent Bayesian posterior probabilities. Values on the time scale are shown as million years before present. North Atlantic land bridge interval is indicated with a grey bar (maximum duration). Tr/J, Triassic/Jurassic extinction.

Ultimately, the Northern Hemisphere radiation of multituberculates and tribosphenic mammals was offset by losses of many archaic mammaliamorph groups during the mid-Cretaceous, including some of the longest-lived mammaliamorph subclades: tritylodontids, docodonts, haramiyidans, plagiaulacidan multituberculates and reduced numbers of triconodonts and 'symmetrodonts'[1]. *Cifelliodon* supports the premise that large-bodied mammaliamorphs of diverse ecologies were present in North American communities up until this mid-Cretaceous diversity bottleneck. Our discovery of *Cifelliodon* and ongoing fieldwork in the Lower Cretaceous of Utah strengthen the hypothesis that corridors of Pangaea-wide dispersal were accessible to relictual clades of large and small vertebrates at least as recently as the Early Cretaceous[27,28].

Consequently, the enigma of why some groups were better at dispersing than others (for example, the conspicuous absence of African multituberculates, an otherwise prolific clade) is more likely to be a consequence of collecting biases or unknown biotic factors rather than strictly tectonic controls or ocean barriers.

Online content

Any Methods, including any statements of data availability and Nature Research reporting summaries, along with any additional references and Source Data files, are available in the online version of the paper at https://doi.org/10.1038/s41586-018-0126-y.

Received: 29 November 2017; Accepted: 10 April 2018;
Published online 23 May 2018.

1. Grossnickle, D. M. & Polly, P. D. Mammal disparity decreases during the Cretaceous angiosperm radiation. *Proc. R. Soc. B* **280**, 20132110 (2013).
2. Hahn, G., Sigogneau-Russell, D. & Wouters, G. New data on Theroteinidae—their relations with Paulchoffatiidae and Haramiyidae. *Geol. Paleontol.* **23**, 205–215 (1989).
3. Butler, P. M. Review of the early allotherian mammals. *Acta Palaeontol. Pol.* **45**, 317–342 (2000).
4. Luo, Z.-X., Gatesy, S. M., Jenkins, F. A. Jr, Amaral, W. W. & Shubin, N. H. Mandibular and dental characteristics of Late Triassic mammaliaform *Haramiyavia* and their ramifications for basal mammal evolution. *Proc. Natl Acad. Sci. USA* **112**, E7101–E7109 (2015).
5. Butler, P. M. & Hooker, J. J. New teeth of allotherian mammals from the English Bathonian, including the earliest multituberculates. *Acta Palaeontol. Pol.* **50**, 185–207 (2005).
6. Zheng, X., Bi, S., Wang, X. & Meng, J. A new arboreal haramiyid shows the diversity of crown mammals in the Jurassic period. *Nature* **500**, 199–202 (2013).
7. Zhou, C. F., Wu, S., Martin, T. & Luo, Z.-X. A Jurassic mammaliaform and the earliest mammalian evolutionary adaptations. *Nature* **500**, 163–167 (2013).
8. Meng, J., Bi, S., Zheng, X. & Wang, X. Ear ossicle morphology of the Jurassic euharamiyidan *Arboroharamiya* and evolution of mammalian middle ear. *J. Morphol.* **279**, 441–457 (2018).
9. Bi, S., Wang, Y., Guan, J., Sheng, X. & Meng, J. Three new Jurassic euharamiyidan species reinforce early divergence of mammals. *Nature* **514**, 579–584 (2014).
10. Han, G., Mao, F., Bi, S., Wang, Y. & Meng, J. A Jurassic gliding euharamiyidan mammal with an ear of five auditory bones. *Nature* **551**, 451–456 (2017).
11. Luo, Z.-X. et al. New evidence for mammaliaform ear evolution and feeding adaptation in a Jurassic ecosystem. *Nature* **548**, 326–329 (2017).
12. Meng, Q.-J. et al. New gliding mammaliaforms from the Jurassic. *Nature* **548**, 291–296 (2017).
13. Rowe, T. B. *Osteological Diagnosis of Mammalia, L. 1758, and its Relationship to Extinct Synapsida*. PhD thesis, Univ. California, Berkeley (1986).
14. Sigogneau-Russell, D. First evidence of Multituberculata (Mammalia) in the Mesozoic of Africa. *Neues Jahrb. Geol. Paläontol. Abh.* **1991**, 119–125 (1991).
15. McDonald, A. T. et al. New basal iguanodonts from the Cedar Mountain formation of Utah and the evolution of thumb-spiked dinosaurs. *PLoS ONE* **5**, e14075 (2010).
16. Gingerich, P. D. & Smith, B. H. in *Size and Scaling in Primate Biology* (ed. Jungers, W. L.) 257–272 (Plenum, New York, 1984).
17. Millien, V. & Bovy, H. When teeth and bones disagree: body mass estimation of a giant extinct rodent. *J. Mamm.* **91**, 11–18 (2010).
18. Krause, D. W. et al. First cranial remains of a gondwanatherian mammal reveal remarkable mosaicism. *Nature* **515**, 512–517 (2014).
19. Krause, D. W., Wible, J. R., Hoffmann, S., Groenke, J. R., O'Connor, P. M., Holloway, W. L. & Rossie, J. B. Craniofacial morphology of *Vintana sertichi* (Mammalia, Gondwanatheria) from the Late Cretaceous of Madagascar. *J. Vertebr. Paleontol.* **34**, 14–109 (2014).
20. Langevin, P. & Barclay, R. M. R. *Hypsignathus monstrosus*. *Mamm. Species* **357**, 1–4 (1990).
21. Hahn, G. & Hahn, R. New multituberculate teeth from the Early Cretaceous of Morocco. *Acta Palaeontol. Pol.* **48**, 349–356 (2003).
22. Rowe, T. B., Macrini, T. E. & Luo, Z.-X. Fossil evidence on origin of the mammalian brain. *Science* **332**, 955–957 (2011).
23. Macrini, T. E., Rougier, G. W. & Rowe, T. Description of a cranial endocast from the fossil mammal *Vincelestes neuquenianus* (Theriiformes) and its relevance to the evolution of endocranial characters in therians. *Anat. Rec. (Hoboken)* **290**, 875–892 (2007).
24. Luo, Z.-X. et al. Evolutionary development in basal mammaliaforms as revealed by a docodontan. *Science* **347**, 760–764 (2015).
25. Heinrich, W.-D. First haramiyid (Mammalia, Allotheria) from the Mesozoic of Gondwana. *Foss. Rec.* **2**, 159–170 (1999).
26. Anantharaman, S., Wilson, G. P., Das Sarma, D. C. & Clemens, W. A. A possible Late Cretaceous "haramiyidan" from India. *J. Vertebr. Paleontol.* **26**, 488–490 (2006).
27. Brikiatis, L. Late Mesozoic North Atlantic land bridges. *Earth Sci. Rev.* **159**, 47–57 (2016).
28. Dunhill, A. M., Bestwick, J., Narey, H. & Sciberras, J. Dinosaur biogeographical structure and Mesozoic continental fragmentation: a network-based approach. *J. Biogeogr.* **43**, 1691–1704 (2016).
29. Rodrigues, P. G., Ruf, I. & Schultz, C. L. Study of a digital cranial endocast of the non-mammaliaform cynodont *Brasilitherium riograndensis* (Later Triassic, Brazil) and its relevance to the evolution of the mammalian brain. *Palaontol. Z.* **88**, 329–352 (2014).
30. Macrini, T. E., Rowe, T. & Vandeberg, J. L. Cranial endocasts from a growth series of *Monodelphis domestica* (Didelphidae, Marsupialia): a study of individual and ontogenetic variation. *J. Morphol.* **268**, 844–865 (2007).

Acknowledgements We thank R. Irmis, C. Levitt-Bussian and the Natural History Museum of Utah (UMNH); Utah Geological Survey, which funded the excavation and preparation of the specimen; A. R. C. Milner who discovered Andrew's Site (UMNH 1207); Utah Friends of Paleontology and volunteers who helped with excavation; Bureau of Land Management for permission (BLM permit #UTEX-05-031) and site supervision in 2005 under J. Cavin; J. Cavin for initial preparation and S. Madsen for final preparation of the specimen; T. Martin for the *Paulchoffatia* jaw from the Guimarota Mammals Collection (GUI MAM) illustrated in Fig. 2c; E. Hsu, S. Merchant and University of Utah Small Animal Imaging facility, Salt Lake City, for high-resolution X-ray computed tomography scanning; J. Lungmus and A. Neander for additional scanning at the University of Chicago PaleoCT; E. Seiffert (USC) for helpful comments. The specimen is housed at UMNH, Salt Lake City.

Reviewer information *Nature* thanks S. Hoffmann and T. Martin for their contribution to the peer review of this work.

Author contributions J.I.K. conducted fieldwork and oversaw laboratory preparation of the specimen; A.K.H., Z.-X.L. and J.A.S. scanned the specimen using computed tomography; A.K.H. analysed the data and conducted the computed tomography reconstructions; A.K.H. illustrated the specimen, and A.K.H. and Z.-X.L. composed the figures; A.K.H., D.M.G. and Z.-X.L. conducted the phylogenetic analysis; and A.K.H., D.M.G., J.I.K., J.A.S. and Z.-X.L. wrote the manuscript.

Competing interests The authors declare no competing interests.

Additional information
Extended data is available for this paper at https://doi.org/10.1038/s41586-018-0126-y.
Supplementary information is available for this paper at https://doi.org/10.1038/s41586-018-0126-y.
Reprints and permissions information is available at http://www.nature.com/reprints.
Correspondence and requests for materials should be addressed to A.K.H. or Z.-X.L.
Publisher's note: Springer Nature remains neutral with regard to jurisdictional claims in published maps and institutional affiliations.

METHODS

High-resolution X-ray computed tomography. The specimen was micro-CT scanned at the University of Utah's Core Small Animal Imaging facility using a Siemens INVEON micro-CT scanner (aluminium filter and energy settings of 180 kV and 500 μA with a voxel size of 94.2 μm^3). Additional focused scanning was performed at University of Chicago's PaleoCT facility on a custom General Electric Phoenix VTOMEX S 240 to visualize the unerupted ultimate molars (energy settings of 180 kV and 500 μA with a voxel size of 25.3 μm^3). Resulting DICOMs were extracted as image stacks and rendered as 3D models in Avizo 7.0 (Visage Imaging, San Diego, CA).

Phylogenetic methods. The previously published matrix[4,24] was modified to evaluate the relationships between *Cifelliodon* and other Mesozoic mammaliamorphs. In total, 538 morphological characters from 125 mammal and nonmammalian synapsid taxa were analysed using Bayesian inference and maximum parsimony. Characters 1–515 correspond to those from the previously published studies[4,24], characters 516–518 are borrowed from previously published data[18] and characters 519–538 are new. All characters had equal weight and none were ordered. We performed the Bayesian analysis in MrBayes version 3.2.6[31] implementing the standard Mk model for morphological evolution[32] with variable character rates. A log-normal rate distribution was chosen for the evolutionary model because of evidence, which suggested that log-normal distributions may be preferred for morphological datasets[33,34]. We ran the analysis for ten million generations (with the first 25% removed as burn-in) and sampled the posterior distribution every 1,000 generations. To increase the chance of state swapping between chains and to help to reduce the standard deviation of split frequencies (that is, help the runs to converge), the difference in 'temperature' between chains was reduced to 0.06 (from the default setting of 0.10). Parsimony analysis was performed in TNT version 1.1 (tree analysis using new technology)[35]. A heuristic search (random addition sequence with 1,000 replicates) was performed and recovered 1,920 equally most parsimonious trees (tree score = 2,776 steps; consistency index = 0.317; retention index = 0.795). The resulting Bayesian consensus and strict consensus parsimony trees are shown in Extended Data Fig. 9.

Reporting summary. Further information on experimental design is available in the Nature Research Reporting Summary linked to this paper.

Data availability. The specimen is reposited at the UMNH, Salt Lake City, USA, and additional data are reposited online at https://www.morphosource.org/. CT image stacks are available from the corresponding authors upon request. Life Science Identifier (LSID): the new genus and species are registered with Zoobank (http://zoobank.org): urn:lsid:zoobank.org:act:C9D9F344-E058-4E7F-AD58-BAED111F574E.

31. Ronquist, F. & Huelsenbeck, J. P. MrBayes 3: Bayesian phylogenetic inference under mixed models. *Bioinformatics* **19**, 1572–1574 (2003).
32. Lewis, P. O. A likelihood approach to estimating phylogeny from discrete morphological character data. *Syst. Biol.* **50**, 913–925 (2001).
33. Wagner, P. J. Modelling rate distributions using character compatibility: implications for morphological evolution among fossil invertebrates. *Biol. Lett.* **8**, 143–146 (2012).
34. Harrison, L. B. & Larsson, H. C. Among-character rate variation distributions in phylogenetic analysis of discrete morphological characters. *Syst. Biol.* **64**, 307–324 (2015).
35. Goloboff, P. A., Farris, J. S. & Nixon, K. C. TNT, a free program for phylogenetic analysis. *Cladistics* **24**, 774–786 (2008).
36. Hoffmann, S., O'Connor, P. M., Kirk, E. C., Wible, J. R. & Krause, D. W. Endocranial and inner ear morphology of *Vintana sertichi* (Mammalia, Gondwanatheria) from the Late Cretaceous of Madagascar. *J. Vertebr. Paleontol.* **34**, 110–137 (2014).
37. Ruf, I., Luo, Z.-X. & Martin, T. Reinvestigation of the basicranium of *Haldanodon exspectatus* (Mammaliaformes, Docodonta). *J. Vertebr. Paleontol.* **33**, 382–400 (2013).
38. Hahn, G. & Hahn, R. in *Guimarota: A Jurassic Ecosystem* (eds. Martin, T. & Krebs, B.) 97–108 (Dr. Friedrich Pfeil, München, 2000).
39. Kermack, K. A., Mussett, F. & Rigney, H. W. The skull of *Morganucodon*. *Zool. J. Linn. Soc.* **71**, 1–158 (1981).
40. Kielan-Jaworowska, Z., Cifelli, R. L. & Luo, Z.-X. *Mammals from the Age of Dinosaurs: Origins, Evolution, and Structure* (Columbia Univ. Press, New York, 2004).

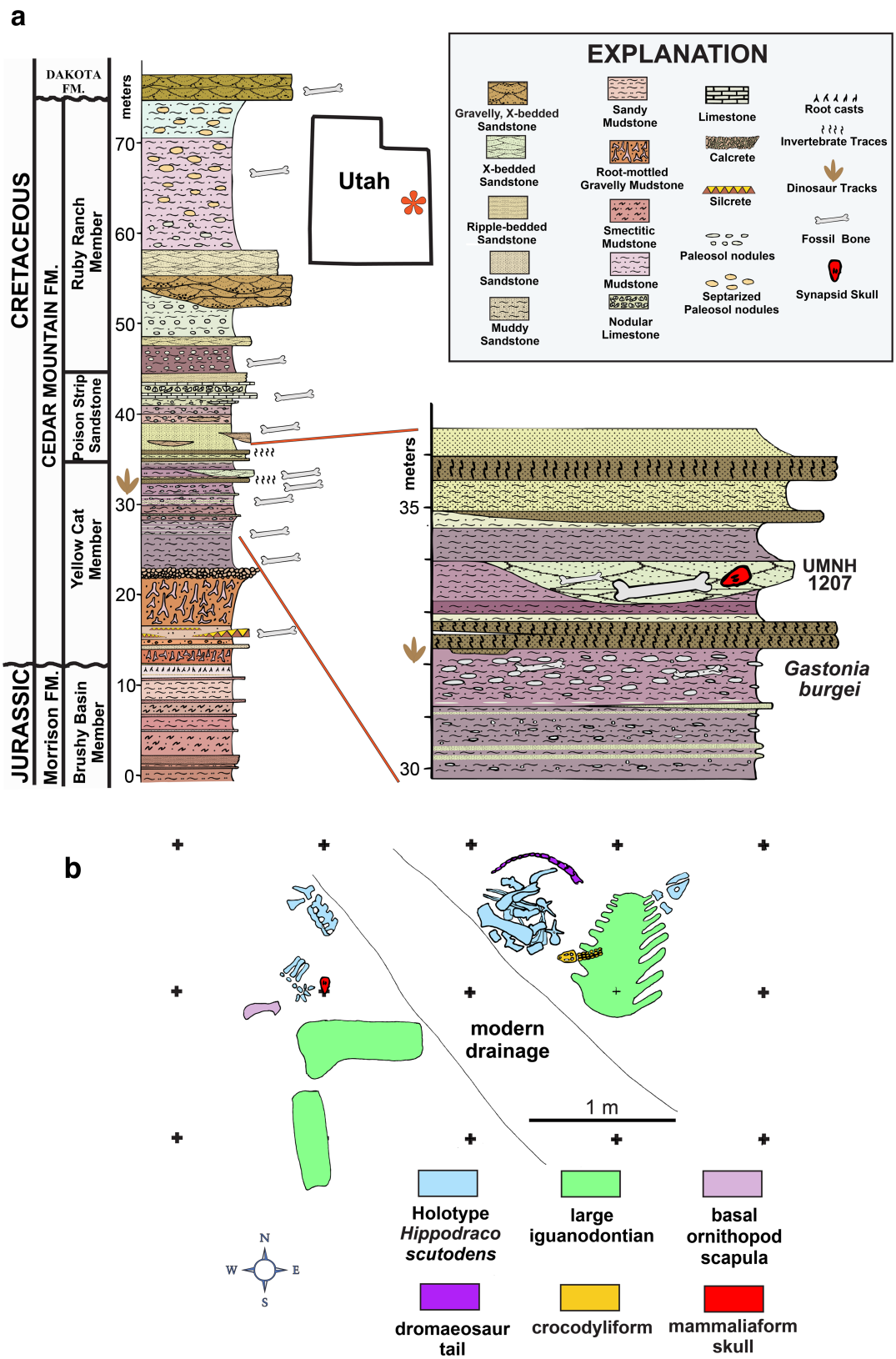

Extended Data Fig. 1 | Stratigraphic section through Andrew's Site and quarry map. a, Revised type section of the Yellow Cat Member of the Cedar Mountain Formation showing the stratigraphic position of Andrew's Site (UMNH 1207). Modified from McDonald et al.[15]. **b**, Quarry map of Andrew's Site. The position of the mammaliaform skull UMNH VP 16771 is indicated in red.

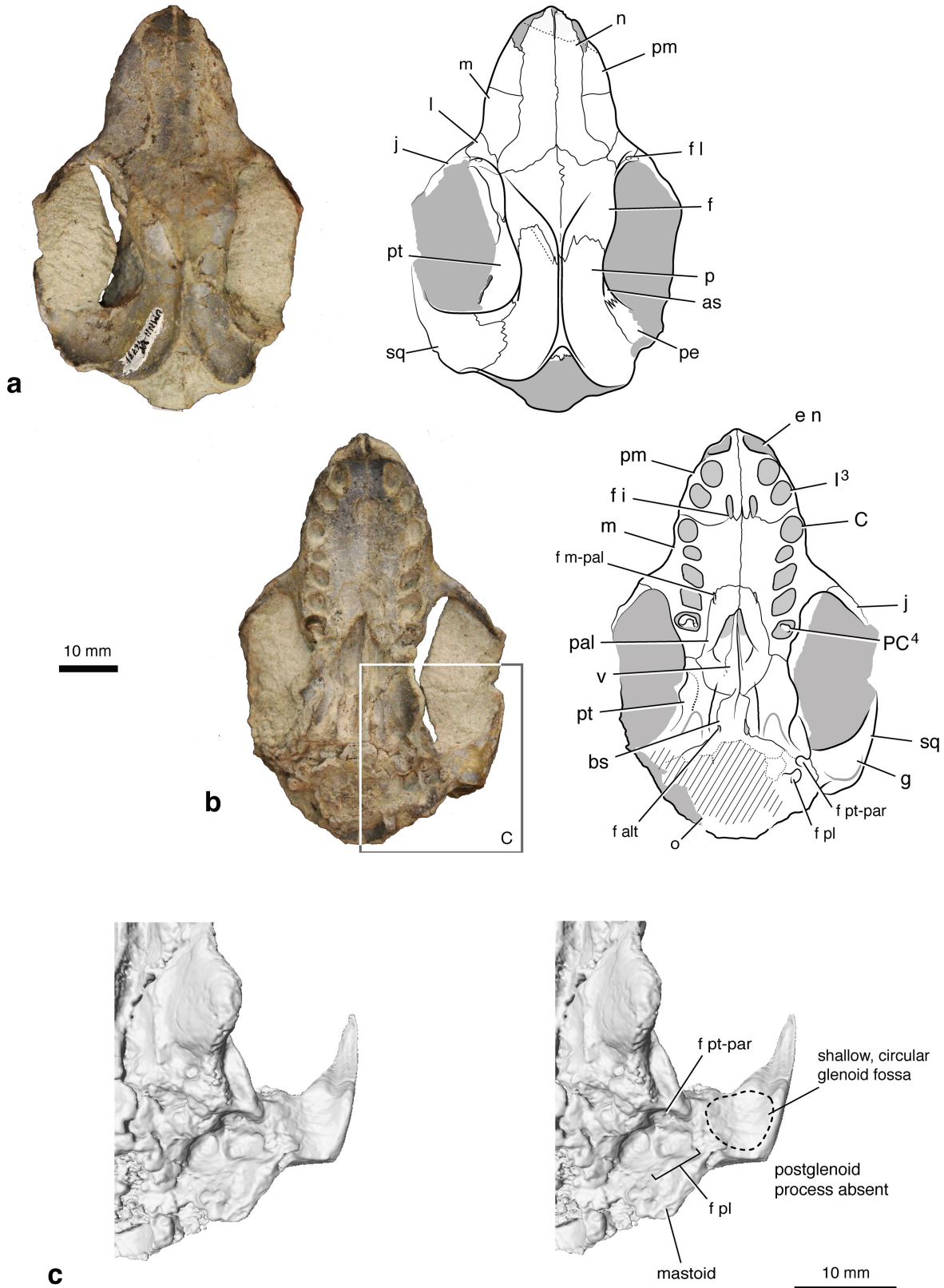

Extended Data Fig. 2 | Skull and interpretive drawings of *C. wahkarmoosuch* UMNH VP 16771. a, **b**, Specimen shown in dorsal (**a**) and ventral (**b**) views. Grey areas represent matrix infill, hatched areas represent crushed/desiccated bones, dashed lines represent cracks through the specimen. **c**, Stereopair of the left side of skull in ventral view to show broad, shallow squamosal glenoid. as, alisphenoid (epipterygoid); bs, basisphenoid; C, upper canine alveolus; e n, external naris; f, frontal; f alt, anterior lateral trough foramen (cavum epiptericum ventral opening); f i, incisive foramen; f l, lacrimal foramen; f m-pal, maxillopalatine foramen; f pl, perilymphatic groove/foramen; f pt-par, pterygoparoccipital foramen; g, squamosal glenoid; I^3, second upper incisor alveolus; j, jugal; l, lacrimal; m, maxilla; n, nasal; o, occipital; p, parietal; pal, palatine; PC^4, in situ posterior upper postcanine (molar); pe, petrosal; pm, premaxilla; pt, pterygoid; sq, squamosal; v, vomer.

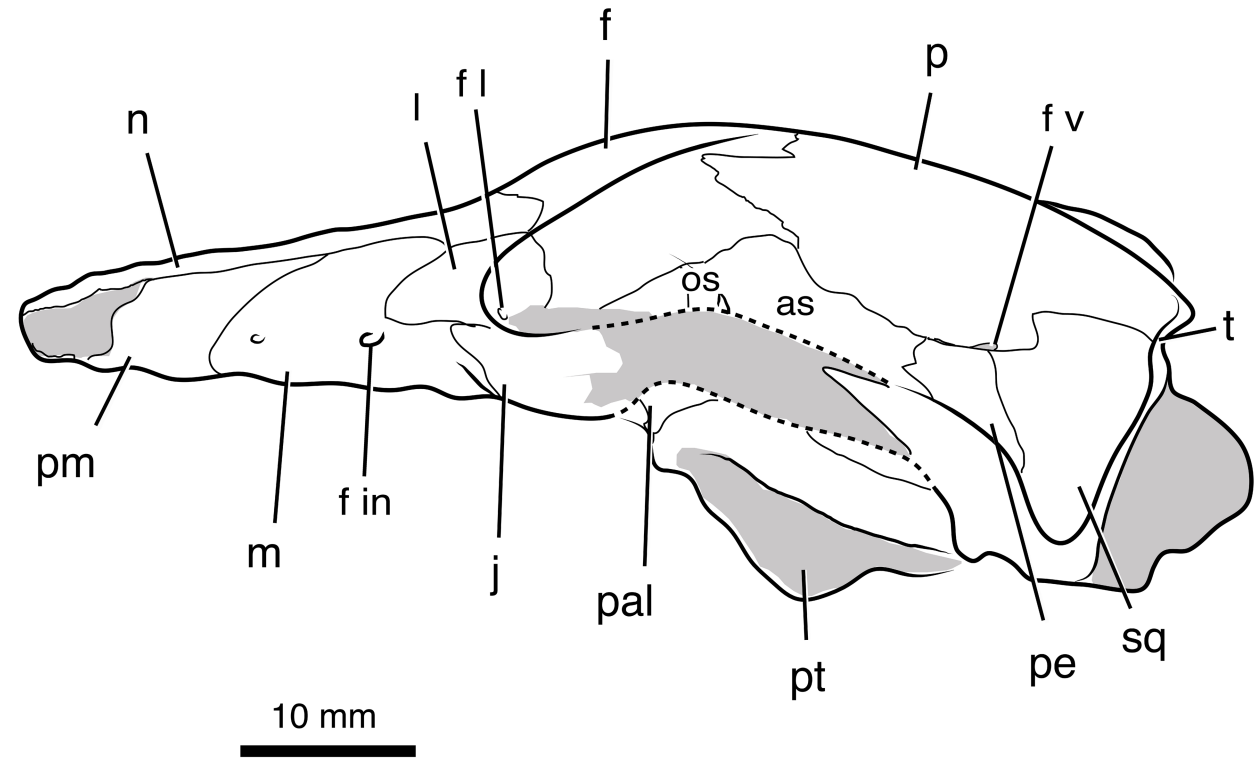

Extended Data Fig. 3 | Skull and interpretive drawings of *C. wahkarmoosuch* UMNH VP 16771 (continued). Specimen shown in left lateral view. Grey areas represent matrix infill, dashed lines represent broken/reconstructed bones. f in, infraorbital foramen; f v, lateral external vascular foramen; os, orbitosphenoid; t, tabular.

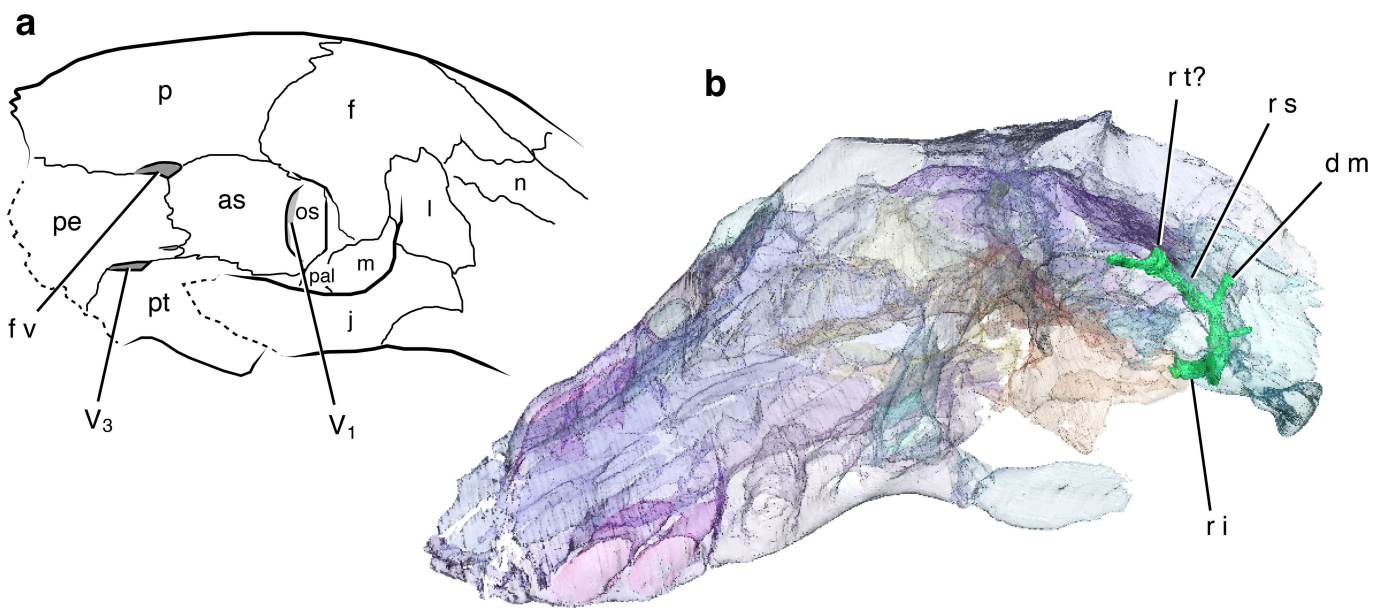

Extended Data Fig. 4 | Cranial foramina and sinuses in the braincase of *C. wahkarmoosuch*. **a**, Line drawing of the posterior skull in right oblique (anterolateral) view. **b**, Computed tomography transparency of the skull in left oblique view, showing the prootic sinus and associated branches of the stapedial artery (light green). d m, diploetica magna; r i, stapedial artery (ramus inferior); r s, stapedial artery (ramus superior); r t, ramus temporalis; V_1, orbital vacuity (hypothesized exit for ophthalmic branch of trigeminal nerve); V_3, foramen pseudovale (hypothesized exit for mandibular branch of trigeminal nerve).

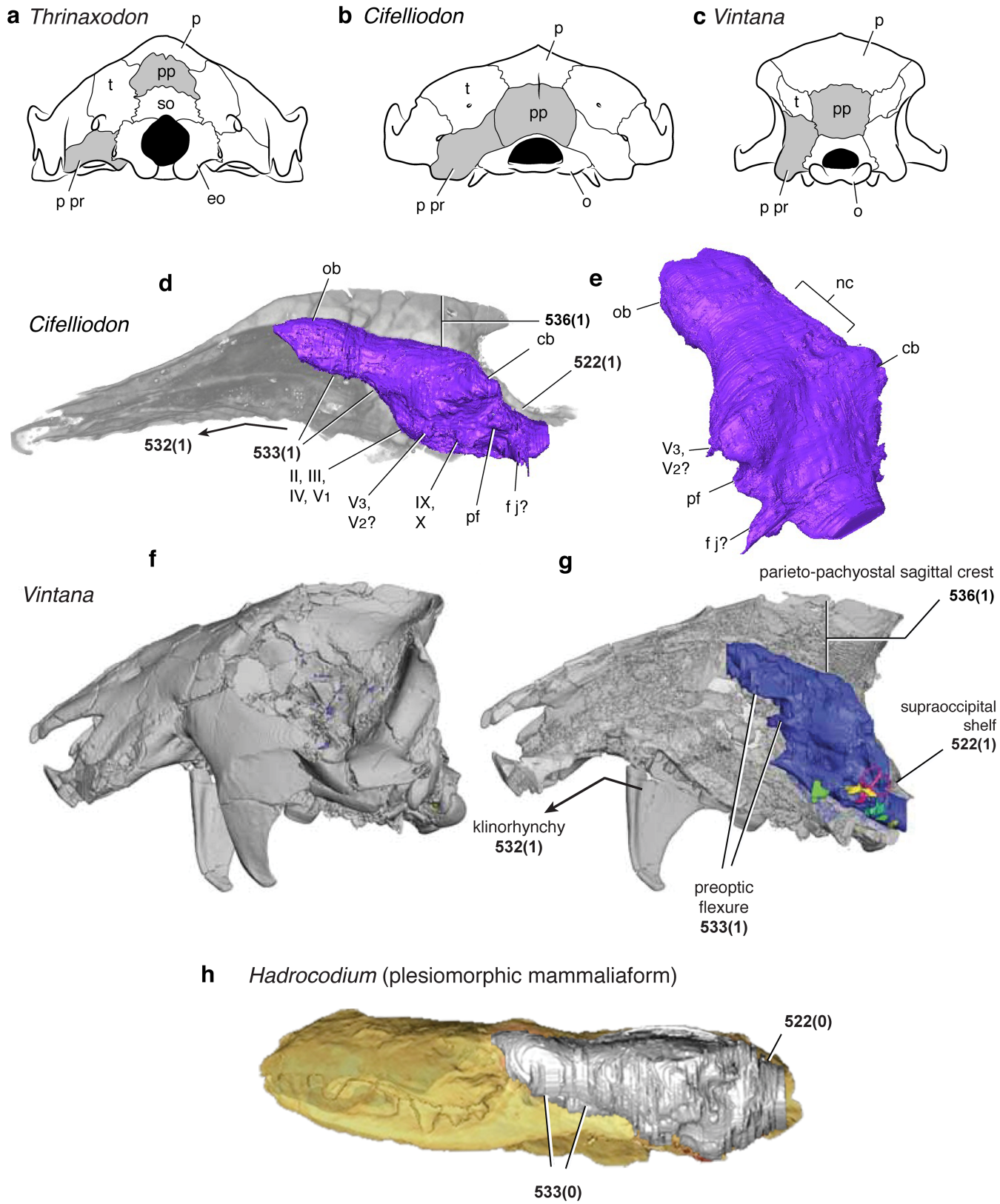

Extended Data Fig. 5 | Cranial vault and endocranial features of *Cifelliodon*. **a**–**c**, Comparison of occiputs of the cynodont *Thrinaxodon liorhinus* (based in part on University of California Museum of Paleontology (UCMP) 40466) (**a**), *C. wahkarmoosuch* (**b**) and *Vintana sertichi* (based on figure 1 of Krause et al.[18]) (**c**). Shaded bones in **b** and **c** emphasize sutural union of postparietal and paroccipital process. Skulls are not shown to scale. **d**–**h**, Brain endocasts. *Cifelliodon* endocast shown in left lateral (**d**) and posterior oblique (**e**) views. Skull of *Vintana* in lateral view shown externally (**f**) and with endocranial features exposed (**g**) (modified from figure 1 of Hoffmann et al.[36] flipped for comparison). Skull of *Hadrocodium* (**h**) shown as a representative plesiomorphic mammaliaform (modified from figure 1 of Rowe et al.[22]; flipped for comparison). Numbers represent characters and character states described in the Supplementary Information. cb, cerebellar hemisphere; eo, exoccipital; f j, cast of jugular foramen within perilymphatic fossa; nc, region of neocortex; ob, olfactory bulb; p pr, paroccipital process; pf, paraflocculus cast; pp, postparietal; so, supraoccipital; II, III, IV, V_1, exit for anterior cranial nerves near sphenorbital fissure; V_3, V_2, roots of mandibular (and maxillary?) branch of trigeminal nerve; IX, X, roots of glossopharyngeal and vagus nerves.

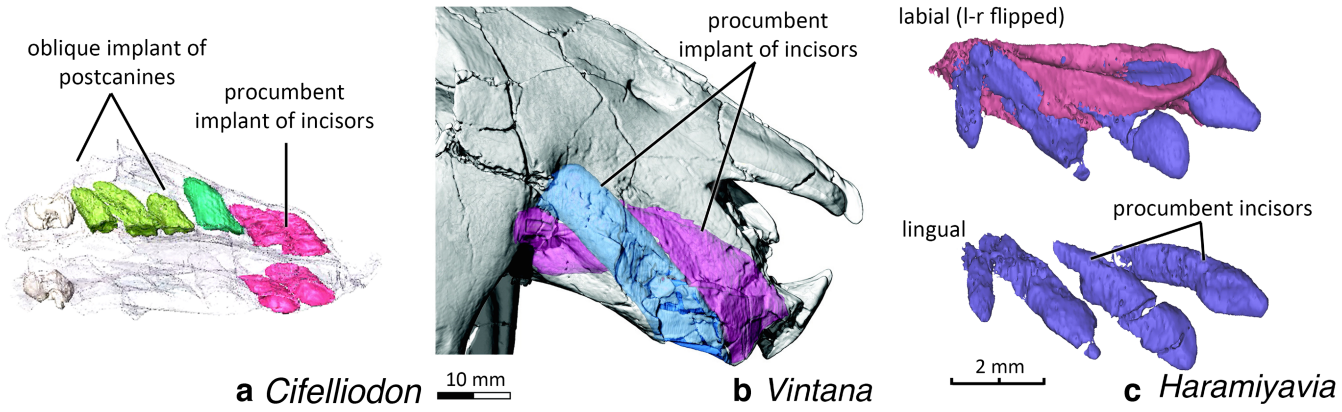

Extended Data Fig. 6 | Derived condition of *Cifelliodon* and other haramiyidans in root morphology and root implant of upper teeth, in contrast to the primitive condition of mammaliaforms. a, *C. wahkarmoosuch* (UMNH VP16771): procumbent implant of incisor roots. **b**, The Madagascar mammaliaform *Vintana* with procumbent incisor roots (based on figure 2 of Krause et al.[18]). **c**, *Haramiyavia*: the first three incisors are procumbent with elongate and procumbent roots (top-labial view, left–right flipped left premaxillary with in situ incisors; bottom-lingual view of left incisors; based on supplementary figure 1 of Luo et al.[4]). **d**, *Morganucodon oehleri* (type specimen, photograph was made by Z.-X.L.): all upper teeth (including incisors) are vertical. **e**, *Haldanodon exspectatus*: upper teeth are all vertical, orientation of incisors shown by their vertical alveoli (resegmented from the previously published dataset[37]). The typical condition for implant of upper teeth is vertical for most mammaliaforms. By comparison the primitive condition of most mammaliaforms, the procumbent incisor implant is a derived condition for haramiyidans, either on all of the incisors (*Cifelliodon* and *Vintana*) or on anterior incisors (*Haramiyavia*).

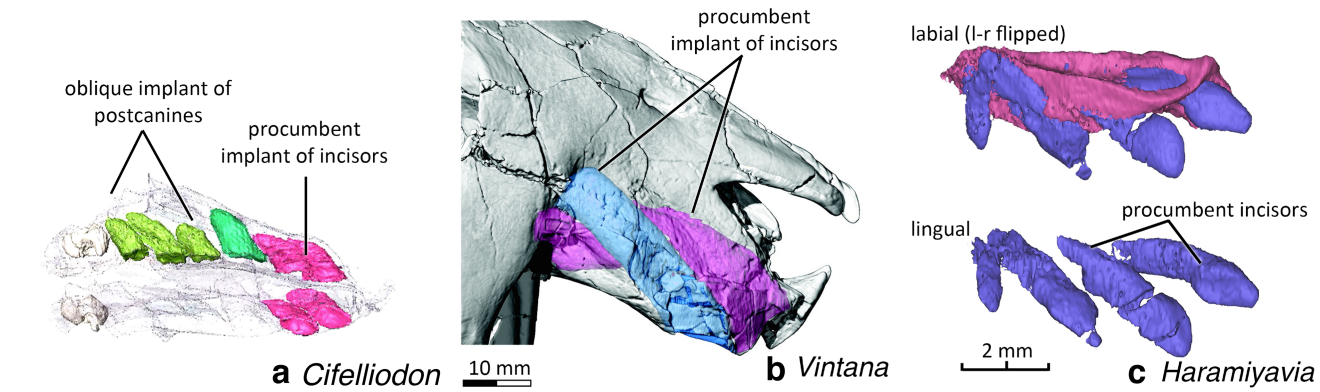

Derived Haramiyidan Condition

Typical Multituberculate Condition

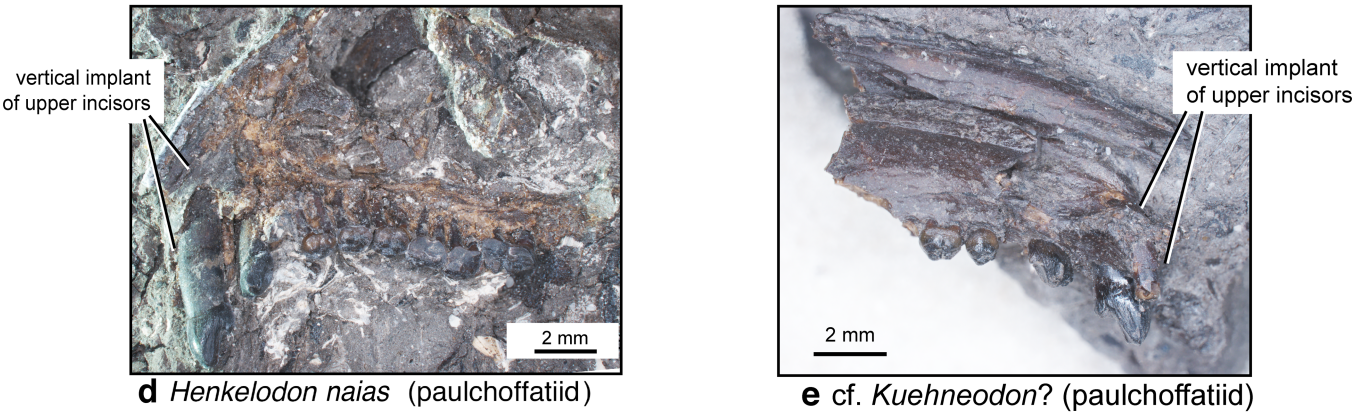

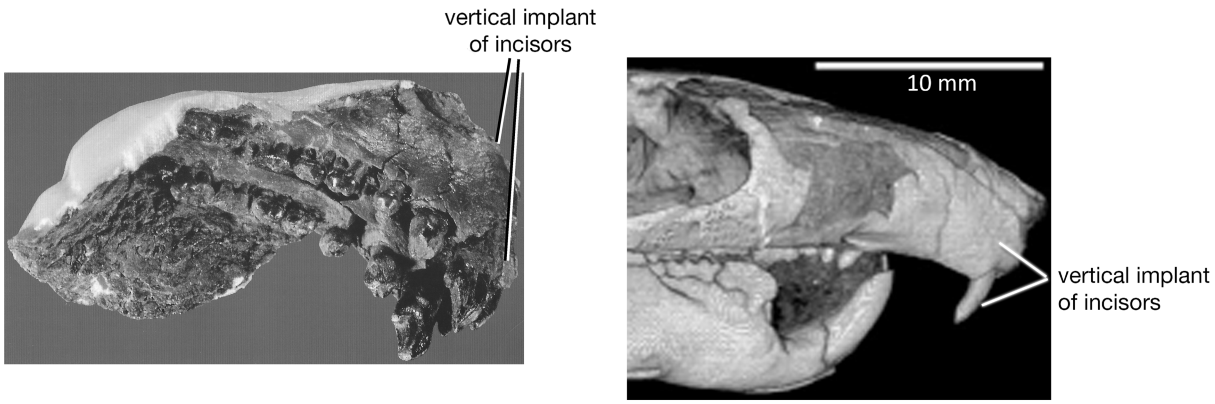

Extended Data Fig. 7 | Derived condition of *Cifelliodon* and other haramiyidans in orientation and implant of incisor and postcanine roots, in contrast to the typical condition of multituberculates (in labial or lingual views). **a**, *C. wahkarmoosuch* (UMNH VP16771): procumbent implant of incisor roots. **b**, *V. sertichi* with procumbent (hypertrophied) incisor roots (based on figure 2 of Krause et al.[18]). **c**, *Haramiyavia*: the first three incisors are procumbent with elongate and procumbent roots (top-labial view, left–right flipped left premaxillary with in situ incisors; bottom-lingual view of left incisors; based on supplementary figure 1 of Luo et al.[4]). **d**, *Henkelodon naias* (Paulchoffatiidae, Multituberculata: GUI-MAM-28-74). **e**, *Kuehneodon dryas* (Paulchoffatiidae, Multituberculata: VJ400-155). **f**, *Kuehneodon simpsoni* (Paulchoffatiidae, Multituberculata; based on figure 12.5 from Hahn & Hahn[38], reproduced with permission). **g**, *Kryptobaatar dashzevegi* (Djadochtatheria; Multituberculata; image from http://digimorph.org/). The procumbent orientation and tooth implant of incisors is a derived condition of haramiyidans (including *Cifelliodon*), in contrast to the vertically implanted incisors and postcanines of most Mesozoic multituberculates, including basal paulchoffatiids, plagiaulacids and djadochtatherians. The vertical implant of incisors in multituberculate condition is plesiomorphic, as it is also shared by other stem mammaliaforms.

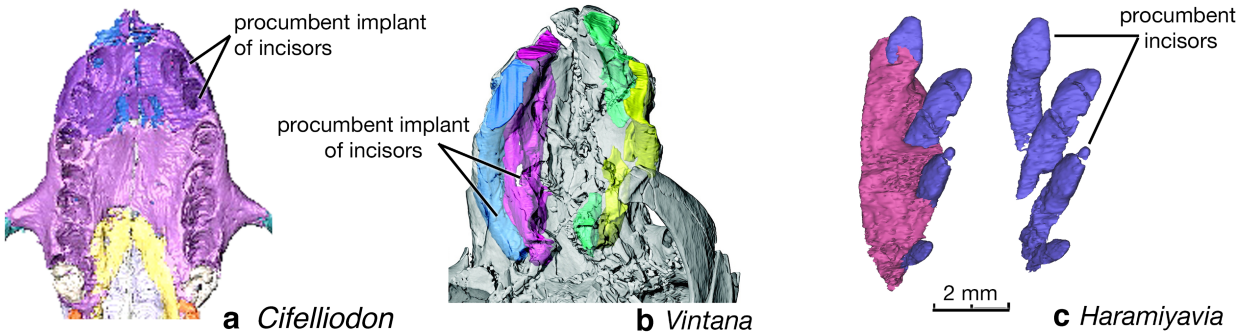

Derived Haramiyidan Condition

Typical Mammaliaform Condition

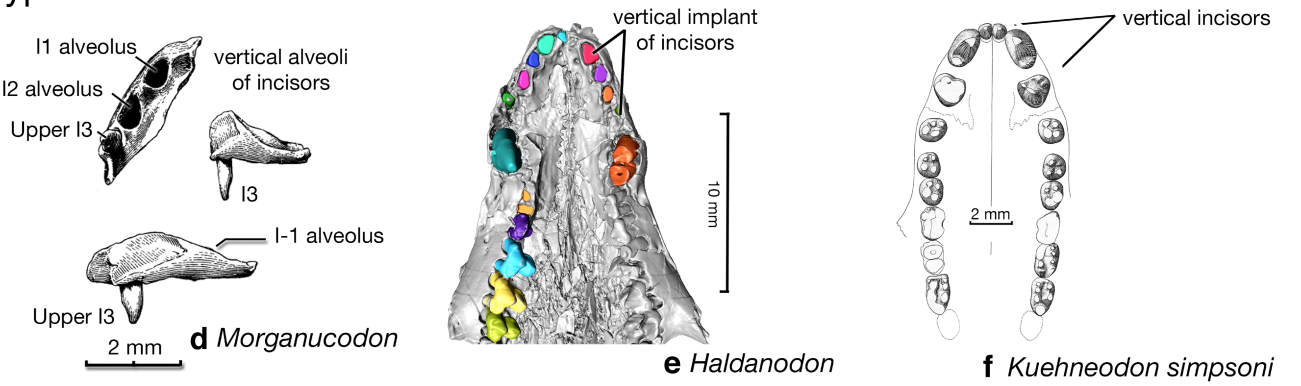

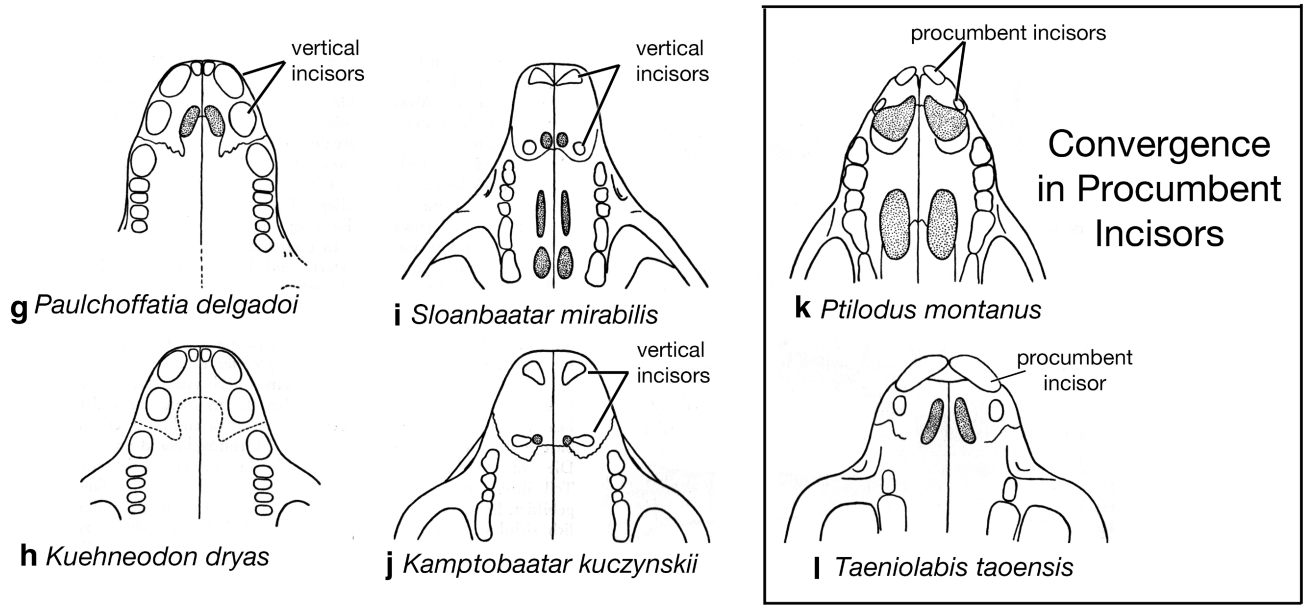

Extended Data Fig. 8 | Derived condition of *Cifelliodon* and other haramiyidan in orientation and implant of incisor roots, in contrast to the typical condition of other stem mammaliaforms and most multituberculates (palatal view). **a**, *C. wahkarmoosuch* (UMNH VP16771): procumbent implant of incisor roots. **b**, *V. sertichi* with procumbent (hypertrophied) incisor roots (based on figure 2 of Krause et al.[18]). **c**, *Haramiyavia*: the first three incisors are procumbent with elongate and procumbent roots (ventral view of left incisors and premaxillary: left with premaxillary; right premaxillary rendered invisible: based on supplementary figure 1 of Luo et al.[4]). **d**, *Morganucodon watsoni* (based on figure 6 of Kermack et al.[39]). **e**, *Haldanodon exspectatus*: vertical orientation of incisors shown by their vertical alveoli (resegmented from the previously published dataset[37]). **f**, *K. simpsoni* (Paulchoffatiidae, Multituberculata) (adapted with permission from Kielan-Jaworowska et al.[40]). **g**, *Paulchoffatia delgadoi* (Paulchoffatiidae, Multituberculata) (adapted with permission from Kielan-Jaworowska et al.[40]). **h**, *K. dryas* (Paulchoffatiidae, Multituberculata) (adapted with permission from Kielan-Jaworowska et al.[40]). **i**, *Sloanbaatar mirabilis* (Djadochtatheria, Multituberculata) (adapted with permission from Kielan-Jaworowska et al.[40]). **j**, *Kamptobaatar kuczynskii* (Djadochtatheria, Multituberculata) (adapted with permission from Kielan-Jaworowska et al.[40]). **k**, *Ptilodus montanus* (adapted with permission from Kielan-Jaworowska et al.[40]). **l**, *Taeniolabis taoensis* (adapted with permission from Kielan-Jaworowska et al.[40]). The procumbent implant of upper incisors is a derived condition for haramiyidans, either on all of the incisors (*Cifelliodon* and *Vintana*) or on anterior incisors (*Haramiyavia*). By comparison, the plesiomorphic condition of incisor implantation is vertical for most stem mammaliaforms (for example, *Morganucodon* and *Haldanodon*). All Mesozoic multituberculates have vertical implant of upper incisors, including basal-most paulchoffatiids that are preserved with upper incisors, plagiaulacids and djadochtatherians. However, the Cenozoic ptilodontid and taeniolabidid multituberculates show procumbent incisors. Because Mesozoic multituberculates have vertical implantation of incisors, the procumbent incisors of ptilodontids and taeniolabidids are interpreted to be secondarily derived and convergent (**k**, **l**).

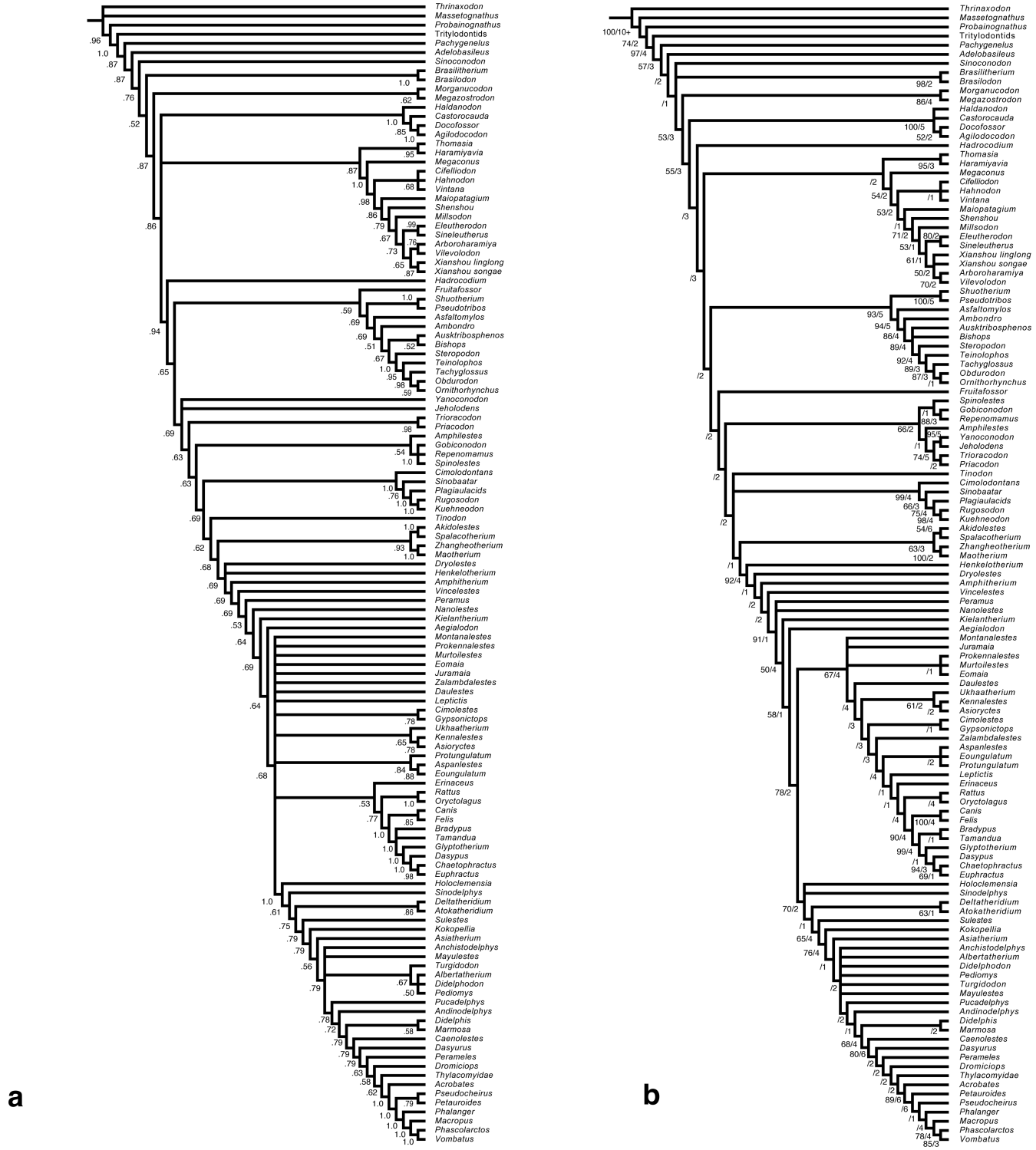

Extended Data Fig. 9 | Phylogenetic results. a, Consensus cladogram from Bayesian analysis in MrBayes 3.2[31]. Branches are not drawn proportional to lengths. Clade support values shown at the nodes are Bayesian posterior probabilities (0.50–1.0). **b**, Strict consensus of 1,920 equally parsimonious trees (tree score = 2,776 steps; consistency index = 0.317; retention index = 0.795) from the parsimony analysis in TNT 1.1[35]. Values at nodes are bootstrap values above 50% (first number (before the solidus)) and Bremer indices (second number (after the solidus)).

Extended Data Table 1 | Major haramiyidan craniodental characters recognized in the present study

Character	Haramiyidae*	*Cifelliodon* (hahnodontid)	*Vintana* (gondwanathere)	Eleutherodontidae‡
Dentition				
occlusal action	orthal and palinal	orthal and palinal	mostly palinal	orthal and palinal
incisor orientation	marked procumbence	marked procumbence	marked procumbence	marked procumbence
upper incisor number	up to four	only two	only two	two or fewer
upper postcanine loci	?	four	up to five	five or fewer
upper premolar number	two or fewer	two or fewer	two or fewer	two or fewer
upper tooth row mesiolateral divergence	?	present	present	?
Skull table				
klinorhynchy	?	present	present	present
tabular bone	?	present†	present†	?
lower canine fossa	?	absent	absent	absent
petrosal-postparietal sutural contact	?	present	present	?
supraoccipital shelf	?	present	present	?
pachyostotic parietal crest	?	present	present	?
Endocranium				
ossified cribiform plate	?	absent†	present?	?
ossified maxilloturbinal bones	?	absent†	absent?†	?
preoptic flexure	?	present	present	?

*Including *Thomasia* and *Haramiyavia*.
†Plesiomorphic retention.
‡Including *Eleutherodon* and *Sineleutherus*, as well as the closely allied *Arboroharamiya*, *Shenshou* and *Xianshou*; 'Euharamiyida' of Bi et al.[9].

nature research

Corresponding author(s): Adam Huttenlocker

Reporting Summary

Nature Research wishes to improve the reproducibility of the work that we publish. This form provides structure for consistency and transparency in reporting. For further information on Nature Research policies, see Authors & Referees and the Editorial Policy Checklist.

Statistical parameters

When statistical analyses are reported, confirm that the following items are present in the relevant location (e.g. figure legend, table legend, main text, or Methods section).

n/a	Confirmed	
☒	☐	The exact sample size (*n*) for each experimental group/condition, given as a discrete number and unit of measurement
☒	☐	An indication of whether measurements were taken from distinct samples or whether the same sample was measured repeatedly
☒	☐	The statistical test(s) used AND whether they are one- or two-sided *Only common tests should be described solely by name; describe more complex techniques in the Methods section.*
☒	☐	A description of all covariates tested
☒	☐	A description of any assumptions or corrections, such as tests of normality and adjustment for multiple comparisons
☒	☐	A full description of the statistics including central tendency (e.g. means) or other basic estimates (e.g. regression coefficient) AND variation (e.g. standard deviation) or associated estimates of uncertainty (e.g. confidence intervals)
☒	☐	For null hypothesis testing, the test statistic (e.g. *F*, *t*, *r*) with confidence intervals, effect sizes, degrees of freedom and *P* value noted *Give P values as exact values whenever suitable.*
☒	☐	For Bayesian analysis, information on the choice of priors and Markov chain Monte Carlo settings
☒	☐	For hierarchical and complex designs, identification of the appropriate level for tests and full reporting of outcomes
☒	☐	Estimates of effect sizes (e.g. Cohen's *d*, Pearson's *r*), indicating how they were calculated
☒	☐	Clearly defined error bars *State explicitly what error bars represent (e.g. SD, SE, CI)*

Our web collection on statistics for biologists may be useful.

Software and code

Policy information about availability of computer code

Data collection	n/a
Data analysis	n/a

For manuscripts utilizing custom algorithms or software that are central to the research but not yet described in published literature, software must be made available to editors/reviewers upon request. We strongly encourage code deposition in a community repository (e.g. GitHub). See the Nature Research guidelines for submitting code & software for further information.

Data

Policy information about availability of data

All manuscripts must include a data availability statement. This statement should provide the following information, where applicable:

- Accession codes, unique identifiers, or web links for publicly available datasets
- A list of figures that have associated raw data
- A description of any restrictions on data availability

The specimen is reposited at the UMNH, Salt Lake City. CT image stacks are available from the corresponding authors upon request. Life Science Identifier (LSID) (http://zoobank.org/ registration): urn:lsid:zoobank.org:act: urn:lsid:zoobank.org:act:C9D9F344-E058-4E7F-AD58-BAED111F574E.

Field-specific reporting

Please select the best fit for your research. If you are not sure, read the appropriate sections before making your selection.

☒ Life sciences ☐ Behavioural & social sciences

For a reference copy of the document with all sections, see nature.com/authors/policies/ReportingSummary-flat.pdf

Life sciences

Study design

All studies must disclose on these points even when the disclosure is negative.

Sample size	n/a
Data exclusions	n/a
Replication	n/a
Randomization	n/a
Blinding	n/a

Materials & experimental systems

Policy information about availability of materials

n/a	Involved in the study
☒	☐ Unique materials
☒	☐ Antibodies
☒	☐ Eukaryotic cell lines
☒	☐ Research animals
☒	☐ Human research participants

Method-specific reporting

n/a	Involved in the study
☒	☐ ChIP-seq
☒	☐ Flow cytometry
☒	☐ Magnetic resonance imaging